MEASURING SLOSHING IMPACTS DURING FULL SCALE TESTS

2 authors:

Edwin van de Bunt
Maritime Research Institute Netherlands

Miroslaw Lech Kaminski
Delft University of Technology

MEASURING SLOSHING IMPACTS DURING FULL SCALE TESTS

E. van de Bunt, MARIN, the Netherlands
M.L. Kaminski, MARIN, the Netherlands

Abstract:

This paper describes the measuring equipment that is used in the first full scale tests on a real membrane containment system subjected to action of breaking waves representative of sloshing impacts in LNG tanks.
The whole test set up for these test is discussed but the focus is on the measurement equipment that is used to capture the wave breaking process before and during the impact using the combination of high speed video cameras and a specially designed optical instrument called the iCAM. The iCAM is a matrix of 640 optical sensors capable to differentiate between solid water, aerated water and air.
The impact of the wave on and the response of the containment system was measured using a data acquisition system which is a high speed, synchronous sampling, single shot type system. A total of 300 sensors including pressure gauges, strain gauges and load cells are measured.
The paper will describe how the pressure sensors were specially selected and explain why they include a special silicone coated membrane with high stiffness. The dynamic calibration process of the pressure sensors is described and is carried out using a specially designed drop test device. Finally, the performance of the measuring equipment during the 110 tests is evaluated.

1. Introduction and background

The Sloshel (Sloshing & Hydro elasticity) project is introduced in the paper by Brosset, Mravak, Kaminski, Collins & Finnigan [1]. Ever increasing demands for operational flexibility in LNG shipping emphasizes the need for accurate prediction of sloshing effects in partially filled LNG tanks. Conventional sloshing assessment of a membrane LNG carrier has been carried out using small-scale (1:30 – 1:60) model tests, combined with numerical simulations. This questions the accuracy of this experimental small scale data and numerical models for these partially filled conditions. To answer these questions full-scale data is needed, with measurements of fluid dynamics as well as the structural response. The Sloshel measurements described in this paper are designed to collect full scale data describing sloshing impacts on a LNG carrier containment system and associated structural response.
MARIN, recognising the need for full-scale validation data, started together with Gaztransport & Technigaz, Bureau Veritas, and Shell an ambitious Joint Industrial Project named Sloshel.
The purpose of Sloshel is to design and perform full scale tests on a containment system in a large flume tank. These tests are designed to reproduce the wave impact conditions that may occur in the tanks of LNG membrane carriers for low and partial fill conditions at full-scale. Ecole Centrale Marseille, American Bureau of Shipping, Chevron, Lloyd’s Register, Det Norske Veritas and Class NK joined the project at a later stage.
The impact waves are generated by a wave-maker in a 240 m long open flume tank using a special focusing method, so that the waves impact on a ‘rigid’ wall on which a fully

instrumented membrane NO96 containment system is mounted together with a rigid concrete block. An extensive database of measurements was gathered during 110 wave impacts successfully carried out by MARIN in the Delta flume operated by Deltares.
The 110 full scale sloshing wave impacts are described in the paper by Kaminski and Bogaert [2].

This paper for the most part focuses on the equipment and measurement systems used to captures not only the effect of the impact with the structural response but also the impacting wave itself. Consequently the complete impact-response relationship is fully recorded.

2. Test Design

The containment system that is tested in this case is the NO96 containment or membrane system. This is mainly a plywood structure with two separate boxes. Each box consist of a plywood cover plate and bottom plate with plywood bulkheads in between. See figure 1 were an instrumented section is shown.

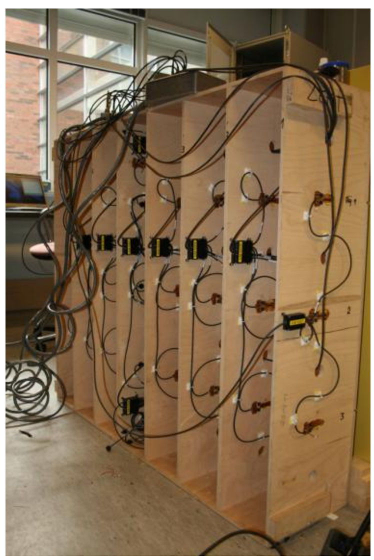

Figure 1: Instrumented section of the NO96 box

In order to investigate the influence of hydro-elastic effects a rigid structure (the concrete block) and the containment system were tested simultaneously assuming that impacts would be predominantly two dimensional, i.e. constant over the flume and test panel width. The set up consisting of the test wall and the test panel with the concrete box and the NO96 box is shown in Figure 2. The test wall is an assembly consisting of the front wall with the test panel, the base wall and three propped support steel beams (brackets). In Figure 3 the test wall is shown after installation in the flume.

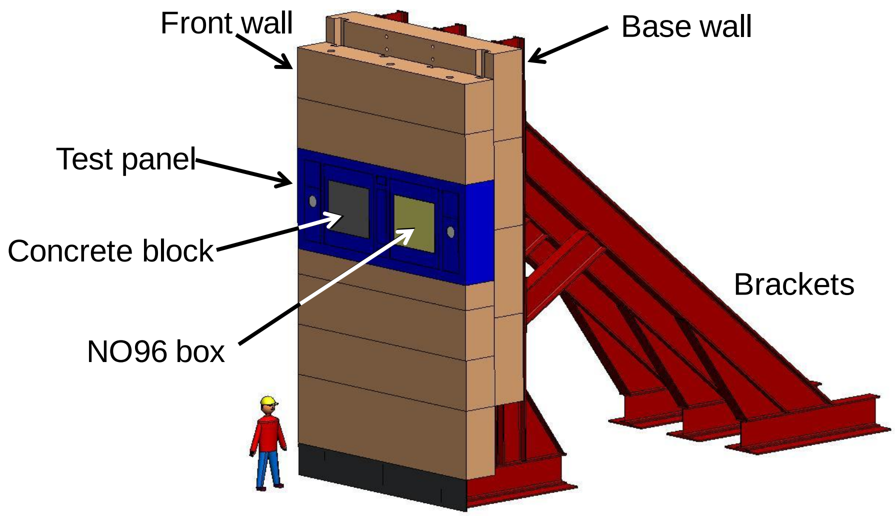

Figure 2: The test wall with the test panel

Figure 3: The test wall in the flume

An important aspect in these experiments is the generation of the impact wave. The wave is generated by generating successive waves of increasing wave length and wave height. Due to the different wave speeds for different wave lengths the all waves will add up to produce a single breaking wave at the focus or focal point. By changing the water depths and by shifting the focal point different types of waves can be generated: aerated, air pocket, flip through and Slosh (see [1] and [2]). Especially the flip through is an important impact type because it gives the highest local pressures on the NO96 box and rigid block.

In Figure 5 an example of an impacting wave is shown.

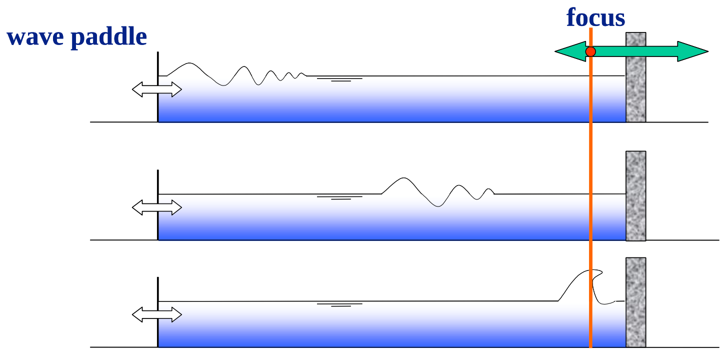

Figure 4: Impact wave generation using wave focusing

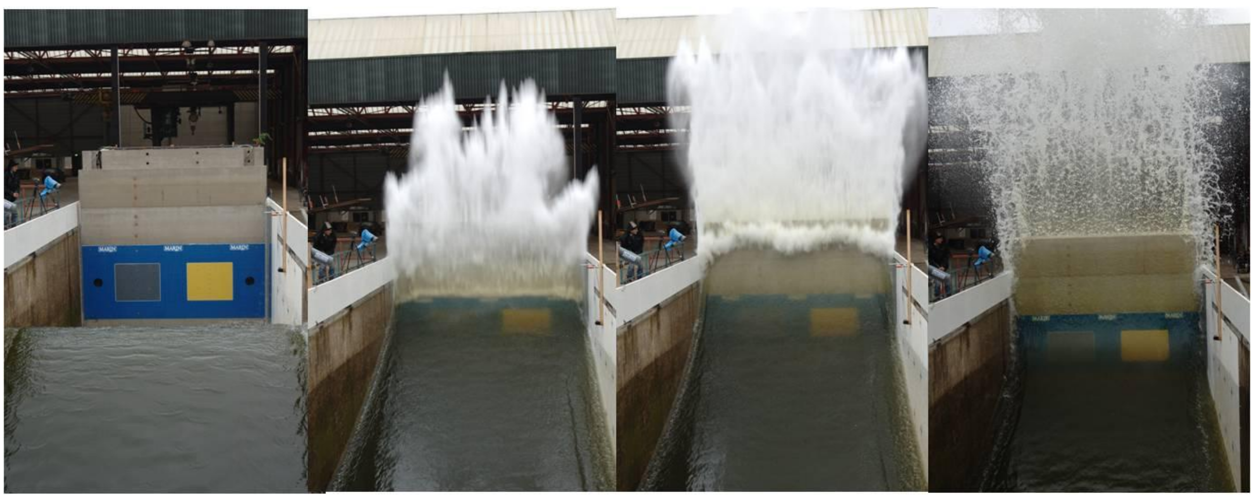

Figure 5: Example of wave impact (Wave S074)

3. The instrumentation

In the following table the instrumentation that is applied during these full scale test is summarized:

	Sensor type	Number of Sensors	Quantity to be determined
Wave	iCAM	640	Impact type
			Water aeration
			Wave velocity
	High speed video cameras	4	Impact type
			Wave velocity
	Wave Probes (Deltares)	3	Wave height
NO96 Box			
Cover plate	Pressure transducers	20	Pressures
	Accelerometers	20	Accelerations, Velocities

	Strain gauges	18	Strains
Primary & Secondary box	Strain gauges	124	Strains
	Accelerometers	24	Accelerations, Velocities
Supporting structure	Load cells	24	Forces
	Accelerometers	5	Accelerations, Velocities
	Load cells	4	Forces on couplers
Concrete Box			
Cover plate	Pressure transducers	20	Pressures
	Accelerometers	20	Accelerations, Velocities
Supporting structure	Load cells	24	Forces
	Accelerometers	5	Accelerations, Velocities
	Load cells	4	Forces on couplers
Test Panel			
	Pressure transducers (Deltares)	2	Pressures
	Accelerometers	3	Accelerations, Velocities
Test Wall			
	Pressure transducers (Deltares)	11	Pressures
	Accelerometers	6	Accelerations, Velocities
	Strain gages	4	Strains in the brackets

The instrumentation is roughly divided in three groups:

1) the pressure transducers to measure the pressures on the cover plate of the NO96 box and the concrete block;
2) the strain gages and accelerometers on the cover plate, bottom plate and bulkheads of the NO96 box to measure the structural response; The strain gages were glued to the plywood. Special care has been taken to assure that the combination strain gage, special glue on the plywood will yield correct strains.
3) the force plates behind the NO96 box and the concrete block to measure the force between the supporting structure and the tested structure.
   The force plate (see Figure 6) is a specially designed structure containing eight triangles where each triangle is supported on three load cells. The NO96 box and concrete block are placed on these force plates using mastic thus enabling to measure the total force.

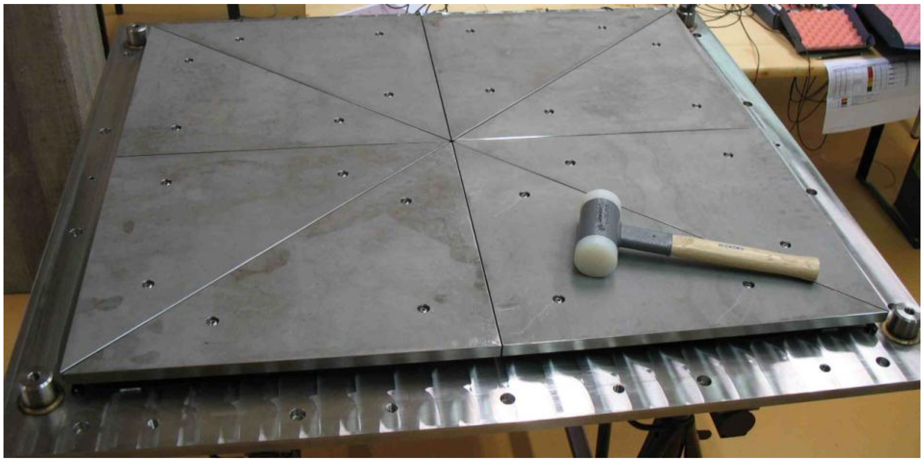

Figure 6: The force plate

4. The Data Acquisition System

The data acquisition system is a robust shock proof system originally designed to be used in crash tests. The system consist of a small pre-conditioner (AIM, see Figure 7) that is installed close to the transducer. This pre-conditioner will condition, filter (anti aliasing filtering) and apply the analogue to digital conversion. The data is sent using a digital protocol to the data collectors that are mounted inside of the test panel. From the data collectors one single Ethernet connection runs to the measurement PC outside of the test panel. A total of 300 AIM's were placed inside of the panel to measure 300 transducers.

Figure 7: The AIM's are positioned close to the strain gages

The data acquisition system is a single shot system. This means that the system when armed, measures continuously but does not record the data on any medium. All data is written in a ring buffer in the data collectors. Any of the 300 channels can trigger the system by surpassing the selected threshold for that channel. At that point the system continues recording data into the ring buffer until the post trigger time is reached. Then the ring buffer is frozen and subsequently the data is transferred to the measurement PC. Using this single shot mechanism a certain time before the measurement (pre-trigger-time) and a certain time after the measurement (post-trigger-time) is stored. The total time stored in the ring buffers is 5 seconds for this configuration. These 5 seconds is more than adequate taken into account that the whole impact takes only a couple of milliseconds. Typically a pre-trigger of one second and a post trigger of three seconds is chosen. The most part of the pre-trigger-time is used to zero the measurement channels to avoid any drift of the transducers between tests. Special care is to be taken that the part that is used for zeroing does not contain a part of the actual signal. The data is later further reduced in the analysis process.

The fixed sample frequency is 50 kHz for all channels. The synchronisation protocol takes care that all measurements are taken simultaneously. The anti-aliasing filtering for the pressure transducers and the strain gages have a cut off frequency at 10 kHz while the accelerometers have a cut off frequency at 4 kHz due to the strong resonance peak at 23 kHz for these specific accelerometers.

5. The iCAM system

The measurement of the impacting wave during the very last moments before the impact is important for the evaluation of the test but it is absolutely essential for the validation of numerical tools. The wave is assumed to be two dimensional during the whole propagation through the flume. A good approach would be to describe the wave using a 2-D profile that develops in time. As the flume walls are made of concrete, it is not possible to observe the wave from the side to provide the wave profile. The solution for this problem is to use a set of high speed video cameras mounted on the side of the flume combined with a specially developed sensor system. The strategy is that the area between one and six meter before the test wall is captured using the high speed video cameras. The last part is measured by a newly developed sensor system. This sensor system is called iCAM (impact CApturing Matrix) and is developed in close co-operation with Optel in the Netherlands.
The actual area measured is from 1.6 m to 0.1 m before the panel over a height of 3 meter. iCAM consists of a 4 panels with each plate containing a grid of 10 by 16 flush sensors of 15mm diameter and internal spacing of 10 cm horizontally and 7.5 cm vertically . The panel is mounted on one of the sidewalls of the flume as close as possible to the test panel (see Figure 8 for the sensor and Figure 9 for the whole set up).

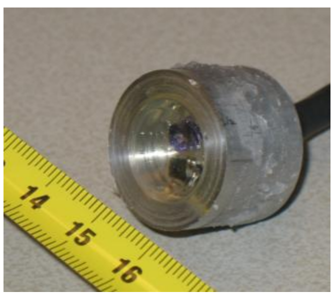

Figure 8: Optical water detection sensor

Figure 9 shows the total iCAM panel containing 40 by 16 sensors in 4 panels of 10 by 16 sensors each. This can also be seen as an image building matrix with a resolution of 40 lines with 16 elements per line giving a total of 640 pixels.

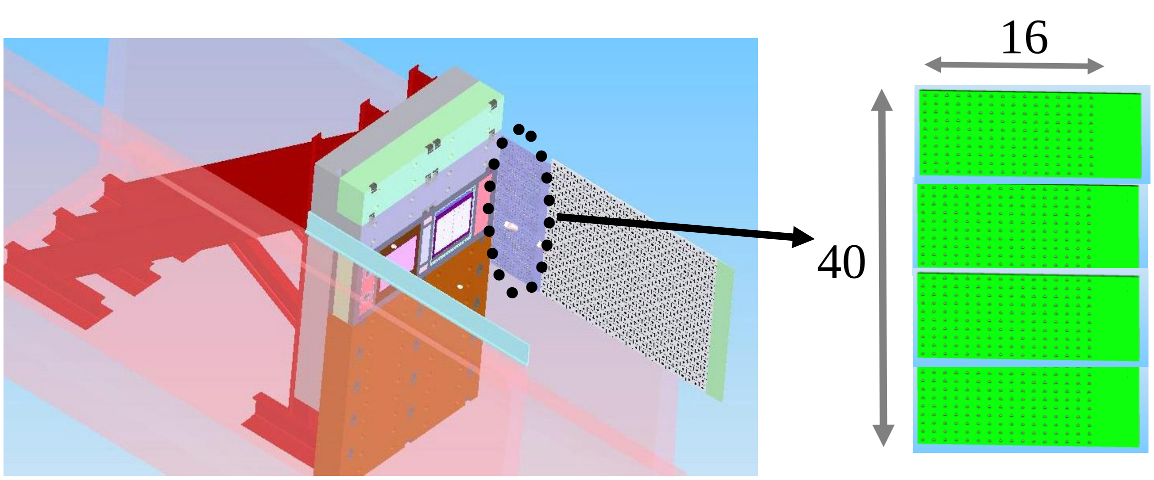

Figure 9: The test wall in combination with the iCAM plates with sensors

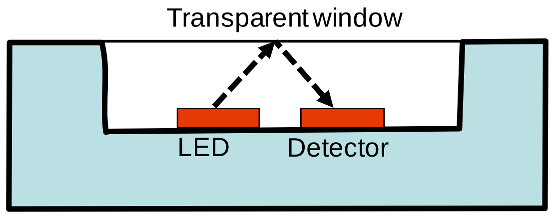

Figure 10: functional iCAM sensor

The iCAM sensor itself consist of two main elements: an infrared light source (LED) and a detector as can be seen in Figure 10. There is no direct optical path from the light source to the detector. The only path is when the light is reflected back to the detector from the window when the sensor is in air. This reflection changes when the window becomes wet: the light is then dispersed and will not reach the detector. The passage of water along the sensor will generate a signal as in Figure 11 with the remark that here the signal is inverted and normalized. The signal during the air/water mixture phase indicates the presence of air bubbles. Each sensor detects the percentage of water coverage and is sampled at a user selectable rate of either 3 kHz or 15 kHz. The response of the sensor is faster than 5 microseconds.

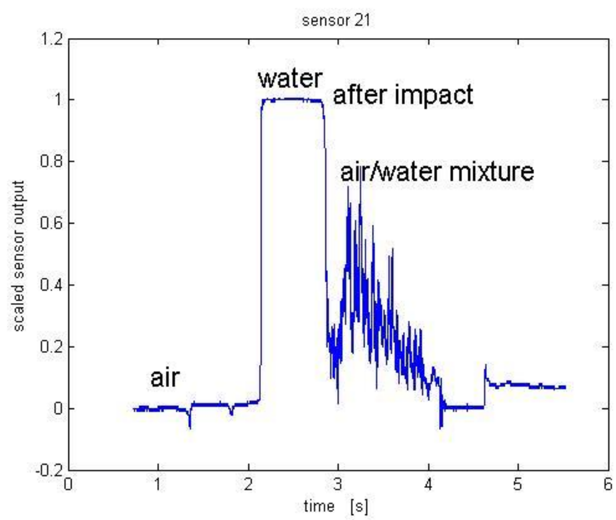

Figure 11: Typical signal from the iCAM sensor during a passing wave

The data from all 640 sensor is combined and processed in the analysis phase, to a series of images in time, more or less comparable to an imaging matrix sensor like the a CCD or CMOS chip. This will provide a sequence of images at a rate of either 3 kHz or 15 kHz. See Figure 12 where one can see the wave just shortly before the impact. The NO96 box is indicated by the black part in the figure ranging from the vertical position of 5 to 6 meter in the test panel. From the images the it can be seen that the two wave components reach each other and meet on the NO96 box clearly indicating this as a “flip through” wave impact type. This type of impact will generate local pressures up until 20 bar which are among the highest pressures measured during the 110 impacts.

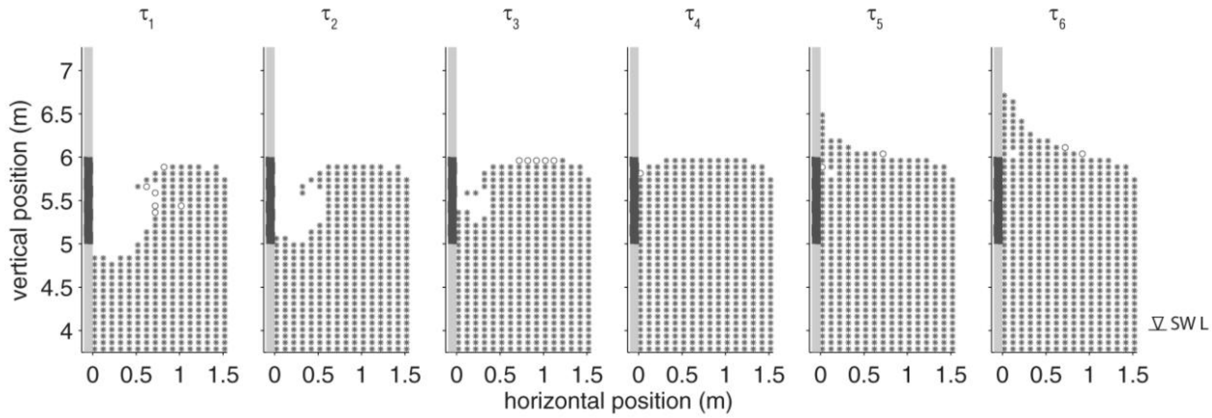

Figure 12: Images from the iCAM sensor: time is progressing from left to right (wave S074, wave shape at six time instants, $\Delta\tau$ = 25 ms)

The measuring time of the iCAM sensor is only one second for the 15 kHz sample rate. Therefore timing is essential. The iCAM system is triggered to start measuring using a water detection sensor that is located some distance above the normal water level and about 6 meter before the test wall. At the moment when a wave passes this sensor will generate a trigger for the iCAM system to start measuring.

6. The high speed video system

Two high speed video cameras are positioned on the side wall of the flume looking down into the flume. Two more cameras are placed in the test panel itself. Figure 13 shows the camera setup and the range covered by the cameras in combination with the iCAM system.
The four cameras are all synchronized and are running at a 100 Hz sample rate. The cameras were set to capture 10 seconds worth of data. They were triggered manually.

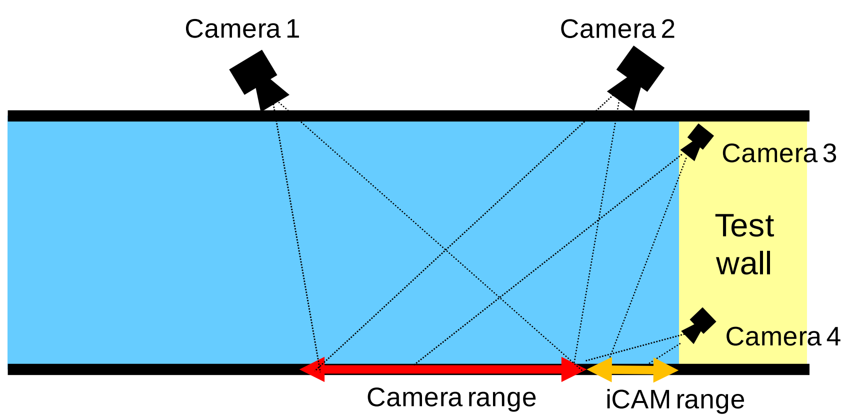

Figure 13: Video camera set up (top view of flume)

After the acquisition of the images they are rectified and are combined to present a 2-D wave front propagating in time. Figure 14 presents the combination of two different camera images in one 2-D wave profile.

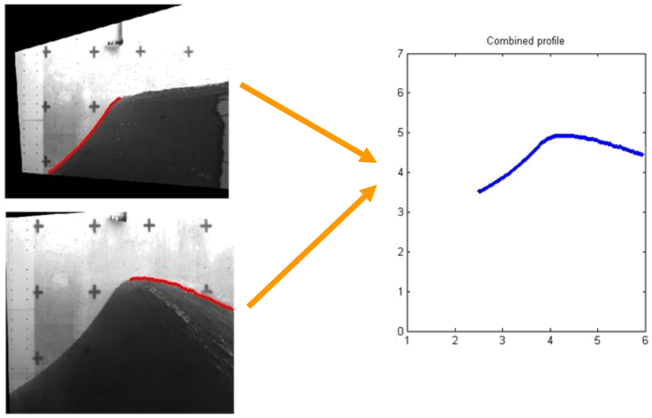

Figure 14: Combining two images in one wave profile

After the construction of the wave profile from the high speed video cameras this profile was combined with the iCAM wave profile to give on smooth wave profile running from six meter before the test wall until the impact on the test wall of the wave. Figure 15 shows two different combined video and iCAM images from a wave impact.

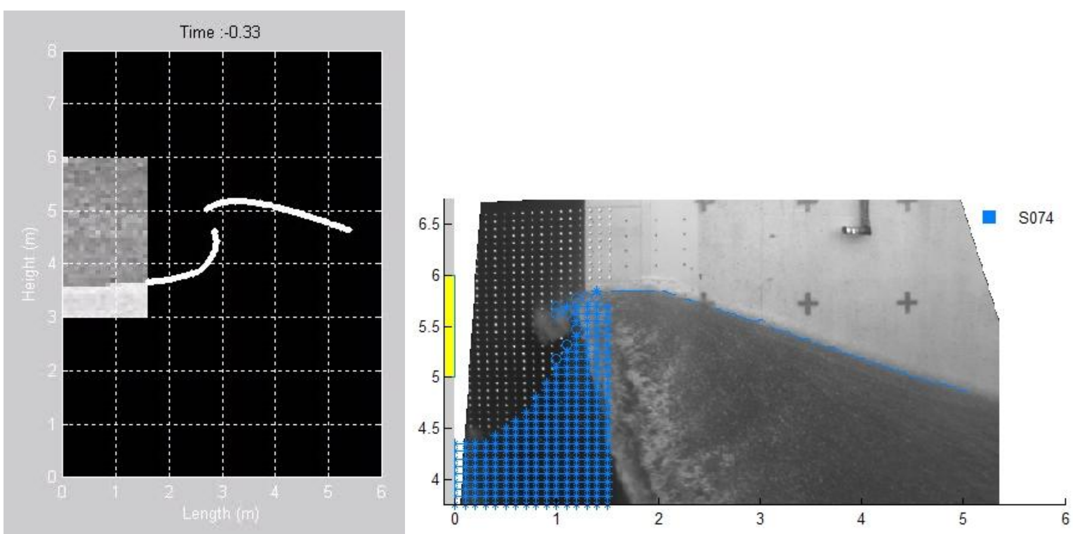

Figure 15: iCAM wave profile and video wave profile combined in one image (two different views)

7. Synchronisation of the different measurement systems

In order to relate the different measurements from the different systems: data acquisition, high speed video system, iCAM and Deltares measurements, to each other, a strict as possible synchronisation was needed. Due to the diversity of the systems a simple hardware

synchronisation was not possible. The iCAM and the data acquisition system are coupled by measuring each other's signals. One iCAM sensor is switched to measure the data acquisition system's trigger. The trigger event is visible in the top left corner of the left iCAM image in Figure 15 near to the 6 meter indication where the a white pixel is visible. The data acquisition system measures on one channel the start of measurement of the iCAM system. This assures a relative tight relationship between these two systems in the range of microseconds. The High speed video is synchronized by a light that is visible in Figure 15 in the top right corner. There two lights are visible: one indicating the trigger from the data acquisition system and one indicating the start of the iCAM measurement. This is off course a rather loose relationship with a maximum error in the order of 10 milliseconds.
Using this diverse set of methods the different measurements are synchronized.

8. Dynamic calibration of pressure transducers

In general a transducer is delivered with a static calibration. This is certainly true for the pressure transducer used in the impact tests. There is no dynamic information available except for the bandwidth of the transducer. Due to the fact that the impacts to be measured in Sloshel are highly dynamic and involve the change of contacting medium form air to water, a special device for the dynamic calibration and testing of pressure transducer was developed at MARIN (See Figure 16).
The drop test device is capable to launch a projectile (i.e. cone) with speeds up to 12 m/s into the water.

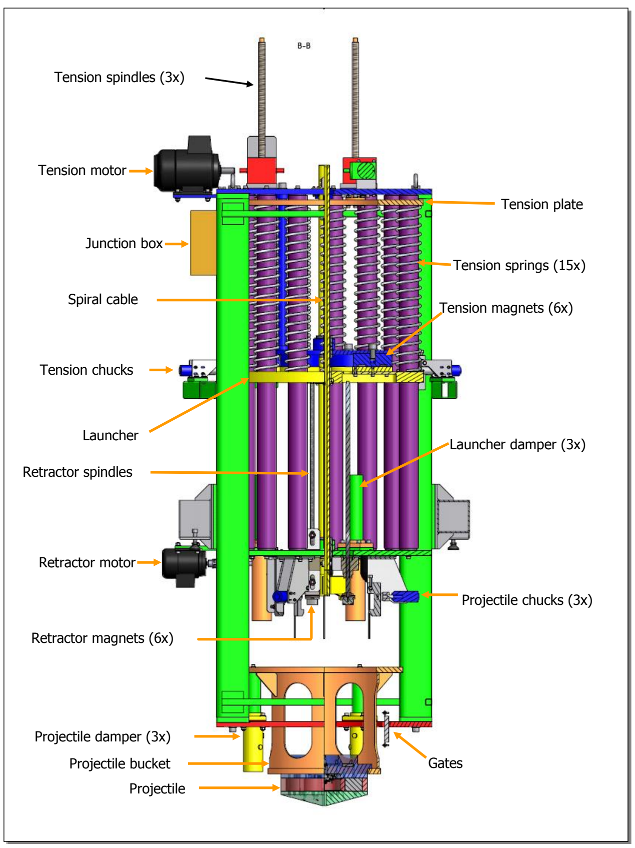

Figure 16: The drop test device with the cone (side view)

After the launch and impact on the water the cone is caught in the bucket and is automatically retrieved for the next test.
The cone is shaped with a dead rise angle of 7.5 degrees, a diameter of 400 mm and a weight of 50 or 75 kilogram (See Figure 17 and Figure 18). The cone accommodates eight pressure transducers, a three axis accelerometer, a water contact sensor and the data acquisition system. The pressure transducers are mounted in a circle with a radius of 100 mm. The pressure transducer has a membrane of 1.3 mm radius and a natural frequency higher than 1 MHz due to the high stiffness of the membrane; full scale pressure range is 100 bar.

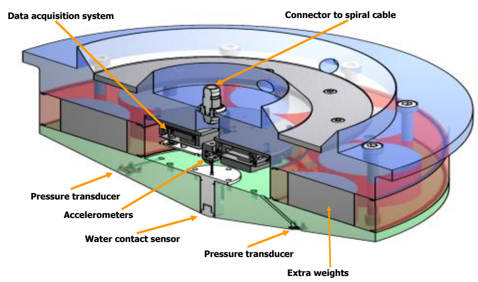

Figure 17: The projectile or cone

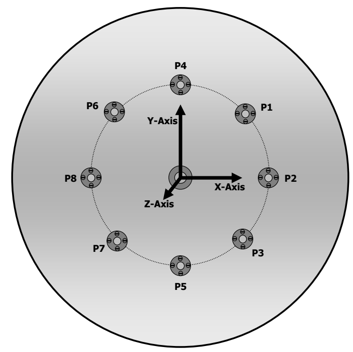

Figure 18: The bottom view of the cone with associated coordinate system

In the following figure a successful launch is shown. Occasionally a high speed video camera is mounted below the point of impact to observe the impact itself. During the damping/receiving phase of the cone in the bucket strong cavitation occurs that has caused some damage to the cone and pressure transducers.

Figure 19: Example of a drop test

The calibration itself is done by comparing the measured pressure pulses to the theoretical model developed by ECM (see [4]) based on the theory derived by Wagner (see [3]). This analytical solution is found for a certain set of parameters: the weight of the cone, the dead rise angle, the inclination of the cone at the impact, the impact velocity and the radius of the pressure transducer.
The measured pressure pulses during these impacts are the result of a number of effects:

- the dynamic effect of the pressure transducer itself,
- the dynamic effect of the fact that the pressure is not constant on the surface but is the result of a passing impulse due to pressure wave moving over the surface of the pressure transducer,
- the analogue conditioner of the data acquisition system specifically the anti-aliasing filter,
- the “limited” sample frequency.

The numerical pulses can only be calculated using a time step of one microsecond or smaller thus resulting in a “sample frequency” of the numerical pulse of 1 MHz or higher. This does not match with the data acquisition system that has a limited sample frequency of 50 kHz. Furthermore a 10 kHz analogue anti aliasing filter is applied prior to the analogue to digital converter. Figure 20 shows the effect of the limited sample frequency. Here the numerical pulse is shown together with four different simulated sample frequencies. Clearly it can be seen that the peak is less higher and wider for decreasing sample frequencies.

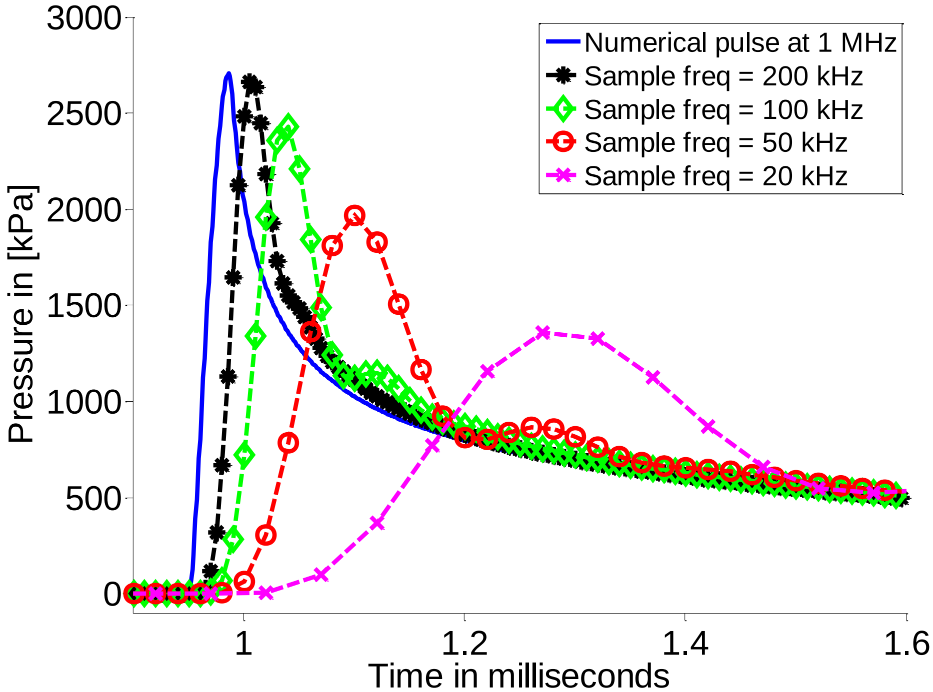

Figure 20: Numerical pulse and sampling effects

In the following figure the theoretical pressure pulse for a point pressure, the theoretical pressure pulse for a real pressure transducer with a finite surface and an actual measured pressure pulse are shown. The measured pulse is here shown with the actual measured points (blue crosses) and the interpolated curve resulting from the interpolation from 50 kHz points to 1 MHz points.

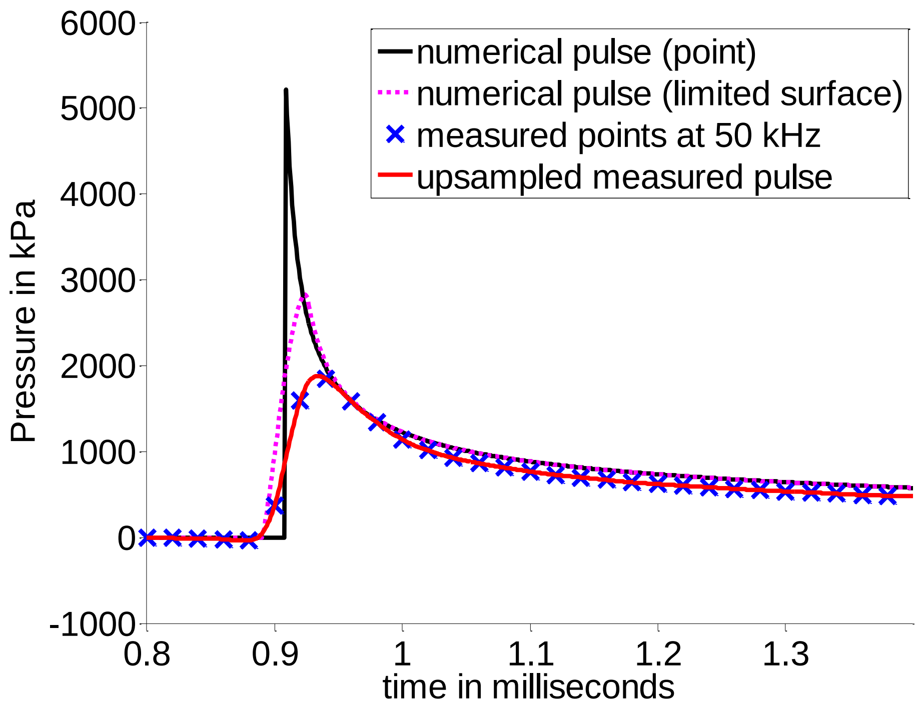

Figure 21: Comparison of numerical and measured pulses

The measured pulse does not quite match the theoretical pulse with limited surface as could be expected. The two pulses can only be compared if the measurements at 50 kHz are interpolated to the “sample frequency” of 1 MHz of the numerical data as can be seen in Figure 22.

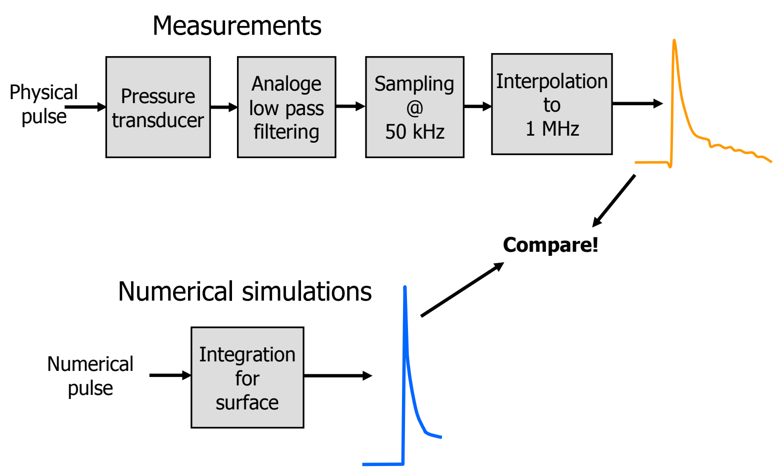

Figure 22: The calibration scheme

The dynamic calibration method now is to estimate the transfer function for the numerical pulse as input and the measured pulse as output. The transfer function is estimated using a state variable representation. Applying the transfer function shows a high correlation between the measured pulse and the transferred numerical pulse. Thus indicating a correct model or transfer function. Using the inverse transfer function the measured pulses can be “corrected” or calibrated. The application of this “dynamic calibration” to the measured pulses in shown in the following figure. The estimated pulse is the result of the dynamic calibration.

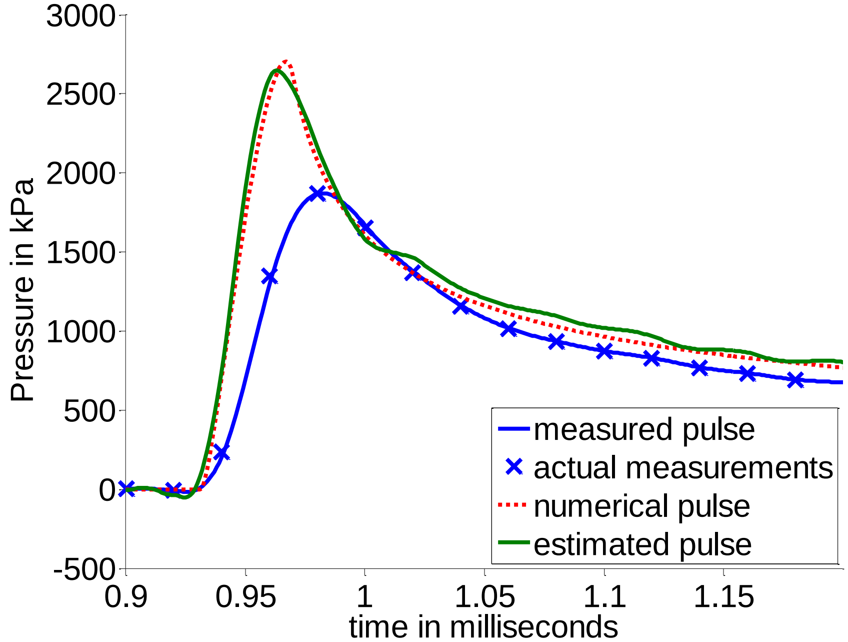

Figure 23: Example of the application of the dynamic calibration

The estimated pulse are points at a sample frequency of 1 MHz. This curve only exist at this sample frequency. When the estimated curve is downsampled or resampled to the sample frequency of 50 kHz the high frequency content disappears and only a curve similar to the measured pulse appears. If one is interested in the absolute pressure peak that occurs in reality it makes sense to use the 1 MHz data because it will give a better representation of the actual impact pulse. One has to keep in mind that the high frequency content is not available in the actual measurement but that it is only added using the dynamic calibration.

The dynamic calibration that is derived here is not only a dynamic calibration for the transducer itself but for the measurement chain “transducer->analoge conditioner->analoge to digital sample process”. This means that always this measurement chain is to be used if the dynamic calibration is to be applied.

Additional spin-off of the drop tests were a rigorous testing of the robustness of the pressure transducers with a relative high failure rate of around 5% during the drop tests. Furthermore during the drop tests the temperature shock due to the rapid immersion in water and acceleration sensitivity of the pressure transducers can be seen. This temperature shock that can be witnessed is the quick mechanical settling of the membrane of the transducer not to be confused with the relatively slow temperature drift of the transducers. The pressure transducers that were ultimately used were relatively insensitive to the temperature shock. This was the result of the silicone coating on the membrane. Any pressure transducer with a stainless steel membrane will show a temperature shock that will be slower than the impacts in the drop tests but will interfere with the wave impacts in the flume.

9. Conclusions

With the test setup and the instrumentation described in this paper the Sloshel consortium has been able to fully capture the full scale hydrodynamic impacts and associated structural response of the NO96 containment system.

With the iCAM the Sloshel team now has a specially developed system with which it is possible to fully capture the wave impact. With the analysis software the wave impact can be classified and better quantified which is crucial for the validation of the numerical tools. In combination with the high speed video observations the wave propagation over the last six meters can be followed. Any deviations from an ideal 2-D wave front can be detected.

The data acquisition system used here is more than adequate for the wave impact measurements but the sample frequency could be higher for the dynamic pressure calibration measurements using the drop test device.

The pressure transducers used in these measurements demonstrated to be robust during the dynamic calibration tests and the wave impact measurements. The temperature shock is not noticeable during the wave impact measurements in the flume. No pressure transducers failed due to the impact of debris or other rubbish which is present in the open air flume.
Using the drop test device a dynamic calibration for the pressure transducers could be determined. The use of it is somewhat limited due to a number of reasons:

1. The “dynamic” effect can only be seen if the data is at the sample rate of 1 MHz. If after the application of the dynamic calibration the data is down sampled to the measurement sample rate of 50 kHz the dynamic effect vanishes.
2. If the pressure data at 1 MHz is compared to the force and strain measurements at 50 kHz there are bound to be dynamic differences due to the different sample frequencies and effective bandwidths. In order to keep these differences to a minimum the data should all be at the same time step or sample rate. In general it is laborious to compare measurement data (at a certain sample rate and with a certain bandwidth limitation) with numerical data with usually a much higher time step and thus sample rate.
3. The pressures during the impact of the cone in the water are not constant on the full surface of the membrane but are building up due to the passing of the wave front over the cone surface and therefore the transducer membrane. The effect is probably small due to the small size of the membrane compared to the wave front speed over the cone and the bandwidth of the measurement channel.

   The pressures during the impacts in the flume for instance during a collapsing air pocket are constant over the membrane of the transducer

The whole test setup described in this paper for the measurements on the NO96 containment system will also be used with some improvements for the measurements on the MARK III containment system in the near future.

10. Acknowledgment

MARIN would like to acknowledge the support provided by the other Sloshel consortium members that have made the Sloshel project possible: American Bureau of Shipping, Bureau Veritas, Ecole Centrale Marseille, Chevron, ClassNK, Det Norske Veritas, Gaztransport & Technigaz, Lloyd's Register and Shell.

11. References

1. Brosset, L., Mravak, Z., Kaminski, M.L., Collins, S. and Finnigan, T. (2009) "Overview of Sloshel project", Proceedings 19th International Offshore and Polar Engineering Conference, ISOPE, 21-26 June 2009, Osaka, Japan, Vol. 3, pp 115-124. www.isope.org.
2. Kaminski, M.L., Bogaert, H., (2009), "Full Scale Sloshing Impact Tests", Proceedings of the 19th International Offshore and Polar Engineering Conference, ISOPE, 21-26 June 2009, Osaka, Japan, Vol. 3, pp 125-134.
3 Wagner, H. „Über Stoß-und Gleitvorgänge an der Oberfläche von Flüssigkeiten." Zeitschrift für Angewandte Mathematik und Mechanik 12 (1932), 192–215.
4 Korobkin A.A. and Scolan, Y.M. (2006), "Three-dimensional theory of water impact. Part 2. Linearized Wagner problem", J. Fluid Mech., vol. 549.